Rheological and Dielectric Behavior of a Styrene−Isoprene−Styrene Triblock Copolymer in *n*-Tetradecane. 1. Rubbery−Plastic−Viscous Transition

Tomohiro Sato, Hiroshi Watanabe,* and Kunihiro Osaki

Institute for Chemical Research, Kyoto University, Uji, Kyoto 611, Japan

Received January 16, 1996; Revised Manuscript Received June 6, 1996[⊗]

ABSTRACT: Rheological and dielectric behavior was examined for a 50 wt % solution of a symmetric styrene−isoprene−styrene (SIS) triblock copolymer (M = 60.2K, S content = 28%) dissolved in an I-selective solvent, *n*-tetradecane (C14). Dynamic mechanical tests with various strain amplitudes, γ_0 = 0.03−0.8, were performed at various temperatures (T). At $T \leq 30$ °C, the system exhibited *elastic*, rubberlike responses characterized with frequency (ω)-insensitive G' being much larger than G'' for small γ_0 and slippage at the measuring assembly wall for large γ_0. At $40 \leq T/°C \leq 80$, the system showed elastic responses (similar to those at $T \leq 30$ °C) for small γ_0 and highly nonlinear, *elastoplastic* responses characterized with lozenge-shaped stress−strain patterns for large γ_0. At $T \geq 90$ °C, *viscous* behavior was observed. These rheological changes were compared with changes in the dielectric behavior of the SIS/C14 system; the I block had dipoles parallel along the chain contour and the motion of its ends was dielectrically detected. In the rubbery regime ($T \leq 30$ °C), no detectable dielectric dispersion was observed, meaning that the I block ends were anchored on rigid S domains. In the viscous regime ($T \geq 90$ °C), prominent dispersion was observed. This dispersion suggested that the I block motion was essentially free from the constraint due to the S domains and the S and I blocks were more or less homogeneously mixed with each other. In the plastic regime ($40 \leq T/°C \leq 80$), the system exhibited onset of dielectric dispersion (upturn of dielectric loss at low ω). This fact suggested some freedom in motion of the I block ends (in the S/I interface) at those T. In the plastic regime, the dielectric response of the SIS/C14 system remained the same at the quiescent state and under oscillatory/steady shear. A previous argument (Watanabe et al. *J. Rheol.* **1984**, *28*, 393) attributed the plasticity to strain-induced motion of the I blocks pulling out the S blocks from softened S domains. However, the shear-insensitive dielectric behavior suggests that the pullout of the S blocks was not the only mechanism providing the plasticity. From this point of view, the mechanism for the plasticity of the SIS/C14 system was discussed in relation to the possible conformations of the I blocks, a bridge connecting different S domains and a loop having two ends anchored on the same domain.

I. Introduction

For A−B−A type triblock copolymers composed of a long B block of low T_g and a relatively short A block of high T_g, elastic, rubberlike behavior is observed at low temperatures (T) while viscous behavior prevails at sufficiently high T.[1−6] This rheological features enables us to use the triblock copolymers as thermoplastic elastomers. From a structural point of view, the rubbery behavior at low T has been attributed to a network structure of glassy, discrete A domains connected with rubbery B blocks, and the viscous behavior at high T, to a more or less homogeneously mixed state (disordered state) of the A and B blocks.

In addition to these well-known rheological responses,[1−6] highly nonlinear, plastic responses were observed at intermediate temperatures for styrene−butadiene−styrene (SBS) triblock copolymers in a B-selective solvent, *n*-tetradecane (C14).[7] In a previous study,[7] this plastic behavior was related to the domain structure in the following way: At intermediate T ($> T_g^{PS}$), the microdomain structure is still preserved but the S domains are in a softened, *liquid* state, enabling the B blocks to pull out the S blocks from the S domains. The S block pulled out from one particular S domain can enter another domain (in a liquid state), enabling the system to flow without macroscopic rupture at $T > T_g^{PS}$. However, during this flow process, the S blocks are brought into enthalpically unfavorable contact with the B blocks (and C14) in the matrix phase. Thus, the S blocks cannot be pulled out and the system deforms only elastically when the applied strain provides mechanical energy smaller than this enthalpic barrier. In other words, the flow takes place only for large strain and/or stress, meaning that the flow is plastic and associated with a yield value that reflects the magnitude of the barrier.

Thus the rheological responses of the triblock copolymer systems should be strongly influenced by the motional freedom for the ends of the middle blocks. It is of our particular interest to experimentally detect the motion of the middle-block ends and compare the results with rheological responses. For this purpose, it is informative to study the rheological and dielectric behavior of styrene−isoprene−styrene (SIS) triblock copolymer systems: Since the I block is chemically similar to B blocks, we expect that the rheological behavior of the SIS system is essentially the same as that of previously studied SBS systems. However, differing from the B blocks, the I blocks have dipole components aligned parallel along the block contour[9−11] (so-called type-A dipoles[8]). For the I block having no inversion of those dipoles, the dielectric relaxation reflects the fluctuations of the end-to-end vector,[8−11] that is, the motion of I block ends; the SIS system should be dielectrically inert at long time scales if the I block ends are fixed on rigid S domains, and vice versa.

On the basis of the above idea, we carried out rheological and dielectric measurements on a 50% SIS/C14 solution and examined the mechanisms and structural origins for the rubbery, plastic, and viscous behavior at low, intermediate, and high temperatures. Specifically, we used the slow dielectric dispersion as a

[⊗] Abstract published in *Advance ACS Abstracts,* August 1, 1996.

S0024-9297(96)00060-5 CCC: $12.00

monitor for the motion of the I block ends in the S/I interfaces and for pulling out of S blocks. The results are presented in this paper.

II. Experimental Section

II.1. Materials. A styrene−isoprene−styrene (SIS) triblock copolymer was synthesized via living anionic polymerization at room temperature. Benzene and *sec*-butyllithium were used as the polymerization solvent and initiator. The polymerization was sequentially carried out in the order S precursor, SI diblock precursor, and SIS copolymer, and the final SIS copolymer anion was terminated with methanol. Some fraction of this copolymer was terminated with a dye, 4-(phenylazo)benzoyl chloride, for a future forced Rayleigh scattering study. Aliquots of the S and SI precursors were taken for molecular characterization. The amounts of these aliquots and the S and I monomers used were carefully adjusted so as to obtain the symmetric SIS copolymer. The resulting PS−PI−PS copolymer was precipitated in methanol to remove (ionic) impurities, freeze-dried from a benzene solution, and stored in a deep freezer until use. A small amount (∼0.05%) of antioxidant, 2,6-di-*tert*-butyl-4-methylphenol, was added to avoid oxidization of the I blocks.

The SIS sample and its precursors were characterized with GPC (HLC-802UR, Tosoh) having a refractive index monitor and a low-angle laser light scattering photometer. The elution solvent was THF, and commercially available monodisperse PS (Tosoh TSK's) were used as elution standards. ^{1}H NMR was used to determine the S/I composition. The weight-average molecular weight and the polydispersity index of the SIS copolymer were $M_w = 60.2 \times 10^3$ and $M_w/M_n = 1.07$. The two PS blocks at the ends had the same molecular weight, $M_w = 8.6 \times 10^3$, and the middle PI block had $M_w = 43 \times 10^3$. The PI block had parallel dipoles aligned in the same direction (without inversion) along the block contour: As explained earlier, motion of the ends of those I blocks is dielectrically detected.

The system examined was a 50 wt % solution of SIS dissolved in *n*-tetradecane (C14; Wako). The solution was prepared by first dissolving a prescribed amount of SIS and C14 in an excess of a common good solvent, benzene, and then allowing the benzene to thoroughly evaporate. (The SIS concentration was determined after complete evaporation of the benzene.) The solvent, C14, is an I-selective solvent and the S blocks formed their domains at low temperatures. The volume fraction of the S domains in the 50 wt % C14 solution was estimated to be smaller than 15 vol %. As judged from extensive structural data on similar copolymer systems,[12] spherical S domains were formed in the solution at strongly segregated states (low temperatures).

II.2. Measurements. Rheological Measurements. Dynamic mechanical measurements were carried out for the SIS/C14 solution at various temperatures ($T = 20-100$ °C) with a laboratory rheometer (RMS605, Rheometrics). To prevent changes in the SIS concentration, the measurements were carried out with a cone-and-plate geometry in a frictionless jacket sealed with pure C14. The cone diameter was 2.5 cm, and the cone angle was 0.1 rad. The amplitude of the oscillatory strain, γ_0, was varied from 0.03 to 0.8.

The stress $\sigma(t)$ against sinusoidal strain $\gamma(t)$ changed with γ_0 in the following way: For sufficiently small γ_0 ($\leq$0.05 or 0.1 for most cases), $\sigma(t)$ was sinusoidal and its amplitude was proportional to γ_0 while its phase difference from $\gamma(t)$ was independent of γ_0. From these linear viscoelastic responses, storage and loss moduli G' and G'' were evaluated.

At $T \leq 30$ °C, the system exhibited slippage at the cone-and-plate wall for larger γ_0 ($\geq$0.2) and moduli could not be evaluated. At higher T, no slippage took place for larger γ_0 but the system exhibited nonlinear responses: At $40 \leq T$ (°C) ≤ 80, $\sigma(t)$ for $\gamma_0 \geq 0.1$ was significantly distorted from the sinusoidal wave and had γ_0-insensitive amplitudes, resulting in lozenge-shaped Lissajous patterns ($\sigma-\gamma$ patterns). For these cases, $\sigma(t)$ were Fourier analyzed to evaluate nonlinear moduli for the jth harmonics[13] G_j' and G_j'' ($j = 1, 3, ...$) and a measure of nonlinearity[13] R_j ($j = 3, 5, ...$) according to eqs 1 and 2.

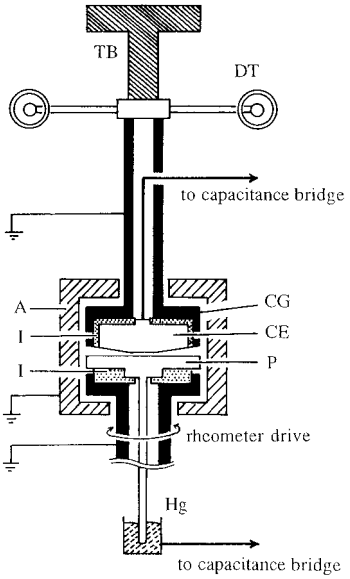

Figure 1. A schematic representation of the rheometer used for dielectric measurements under shear. CE, cone electrode (guarded); P, plate electrode (unguarded); CG, guard for cone electrode; Hg, mercury contact point; I, insulator; A, thermal bath; TB and DT, torsion bar and differential transducer for torque measurements.

$$\sigma(t) = \gamma_0 \sum_{j=\text{odd}} (G_j' \sin j\omega t + G_j'' \cos j\omega t) \tag{1a}$$

$$\gamma = \gamma_0 \sin \omega t \tag{1b}$$

$$R_j = [(G_j')^2 + (G_j'')^2]^{1/2}/[(G_1')^2 + (G_1'')^2]^{1/2} \tag{2}$$

(Even harmonics (j = even) had negligible contribution to $\sigma(t)$.) Note that the nonlinear modulus G_1'' has the same meaning as the linear loss modulus G''; both G'' and G_1'' represent a loss of mechanical energy (dissipated as heat) during one cycle of oscillatory strain.

At 90 °C, $\sigma(t)$ was nearly sinusoidal but the resulting moduli, G_1' and G_1'', were dependent on γ_0. Finally, at 100 °C, the linear viscoelastic behavior was observed in the entire range of γ_0, and G_1' and G_1'' were reduced to the linear moduli, G' and G''.

Dielectric Measurements. Dielectric measurements were carried out with capacitance bridges, GR 1648A (General Radio) and HP 4285A (Hewlett-Packard). The measurements were carried out at the quiescent state, under large-amplitude oscillation, and during steady shear. For this purpose, we used cone-and-plate type electrodes (of cone angle = 2.6°, diameter = 3.0 cm) that were capable of being mounted on a rheometer (Autoviscometer L−III, Iwamoto Seisakusho, Kyoto). This commercially available rheometer was modified to include a mercury contact point (Figure 1), which enabled dielectric measurements under oscillatory/steady shear without mechanical disturbance for the electrical contact.

Determination of T_g^{PS}. Differential scanning calorimetric measurements were carried out with a scanning calorimeter (DSC2910, TA Instruments) to evaluate T_g of the S cores in the SIS/C14 system. The result was $T_g = 34 \pm 4$ °C. This T_g is lower than T_g of bulk PS, indicating that the S cores in the system are swollen with C14.

III. Results

III.1. Characteristic Stress−Strain Patterns. Figures 2−4 show typical Lissajous patterns ($\sigma-\gamma$ patterns) obtained at various temperatures. In each figure, the patterns at (a) low and (b) high ω are

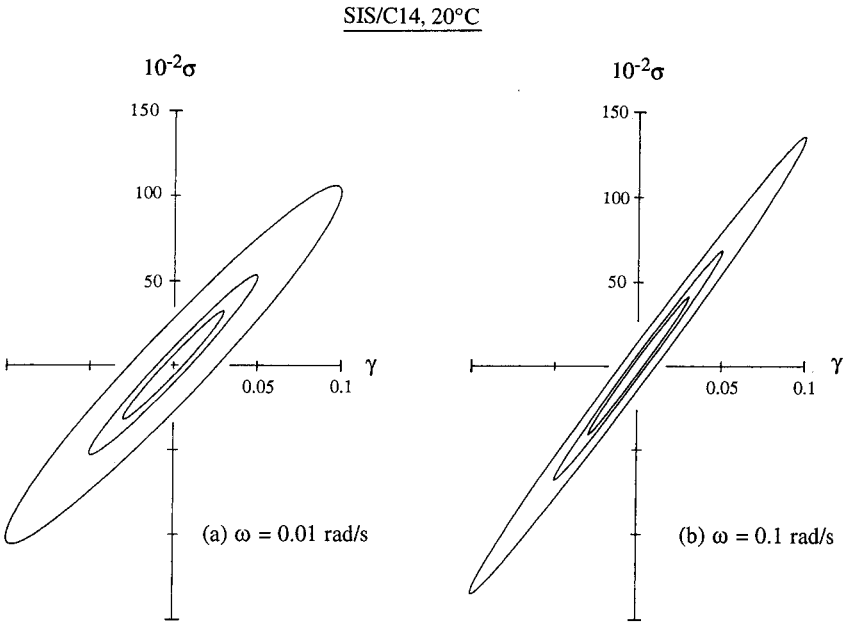

Figure 2. Lissajous patterns ($10^{-2}\sigma$ in units of Pa) at (a) $\omega = 0.01$ rad s^{-1} and (b) $\omega = 0.1$ rad s^{-1} obtained for the SIS/C14 system at 20 °C (rubbery regime).

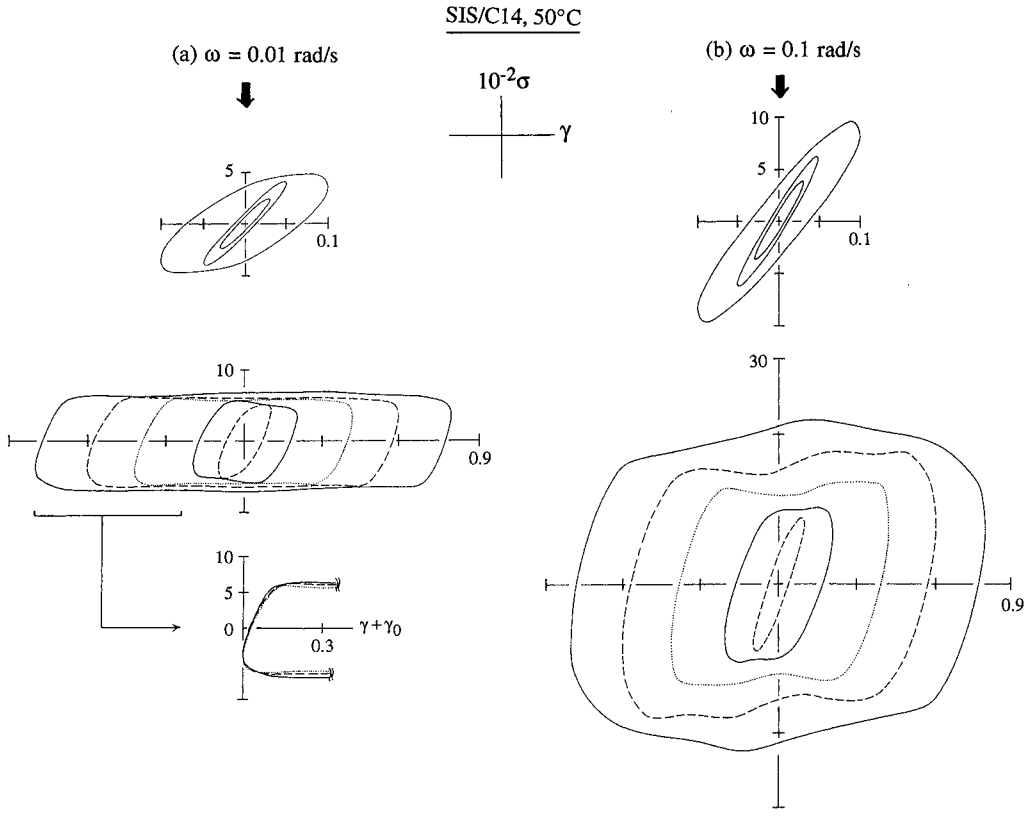

Figure 3. Lissajous patterns ($10^{-2}\sigma$ in units of Pa) at (a) $\omega = 0.01$ rad s^{-1} and (b) $\omega = 0.1$ rad s^{-1} obtained for the SIS/C14 system at 50 °C (plastic regime). The bottom of part a indicates plots of σ against a rescaled strain, $\gamma + \gamma_0$, measured from the γ-reversal point ($\gamma = -\gamma_0$).

compared. The patterns in parts a and b are indicated in the same σ and γ scales ($10^{-2}\sigma$ in units of Pa) so that their differences can be visually noted with ease. In Figures 3 and 4, the patterns obtained for $\gamma_0 \leq 0.1$ and $\gamma_0 \geq 0.1$ are separately shown with different magnifications.

In Figures 2−4, we note different rheological characters at low, intermediate, and high T. At 20 °C (Figure 2), the patterns are elliptic and have only small phase differences between $\gamma(t)$ and $\sigma(t)$ at $\omega = 0.01$ and 0.1 s^{-1}. In addition, the amplitude of $\sigma(t)$ at respective ω is proportional to γ_0, and the resulting G' and G'' ($\ll G'$) are independent of γ_0. Thus, the system exhibits essentially elastic, linear viscoelastic behavior for $\gamma_0 \leq 0.1$. These features, together with slippage at the cone-and-plate wall for larger γ_0, are characteristic of cross-linked rubbers, thereby allowing us to classify the system at 20 °C to be in a rubbery regime.

At 90 °C (Figure 4), the Lissajous patterns at low ω are elliptic and dominated by the out-of-phase component of σ in the entire range of γ_0. At high ω, the patterns are elliptic for small γ_0 (≤ 0.1) but become a

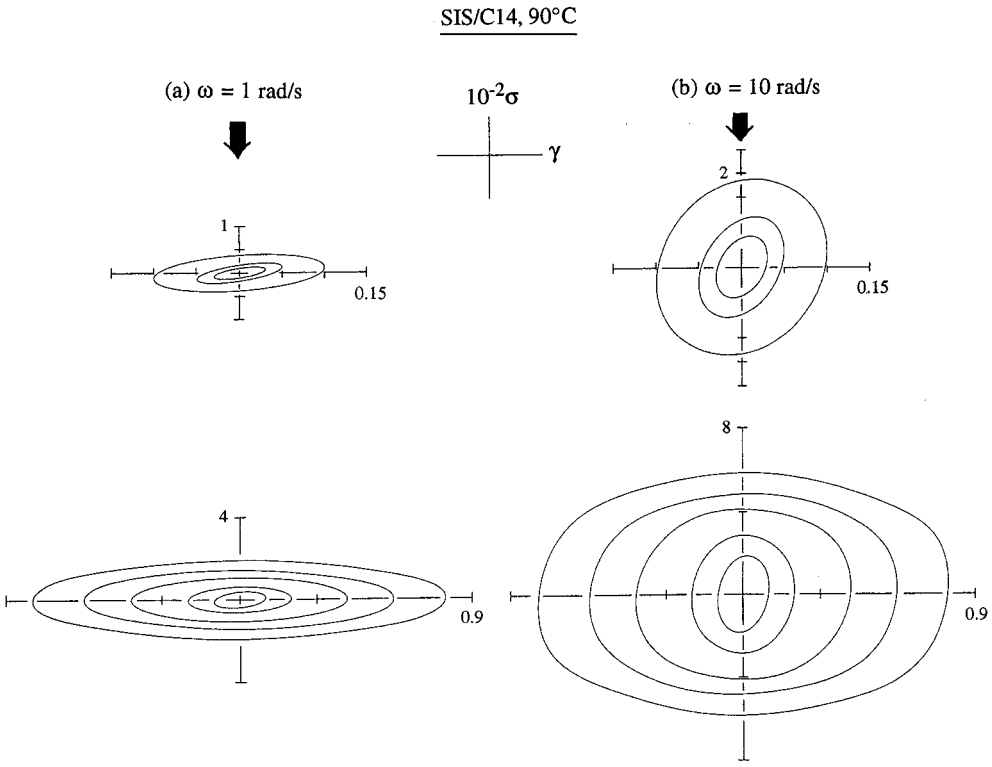

Figure 4. Lissajous patterns ($10^{-2}\sigma$ in units of Pa) at (a) $\omega = 1$ rad s^{-1} and (b) $\omega = 10$ rad s^{-1} obtained for the SIS/C14 system at 90 °C (viscous regime).

little distorted for larger γ_0. The amplitude of $\sigma(t)$ decreases with decreasing ω, as is characteristic of (either linear or nonlinear) viscous fluids. Thus, the system at 90 °C is in a viscous regime. However, the direction of the elliptic axis changes with $\gamma_0 \geq 0.1$ (cf. magnified patterns in part a), and the linear viscoelastic behavior is observed only for small γ_0 ($\leq$0.05). This fact and the small distortion of the patterns at high ω seen for $\gamma_0 \geq 0.1$ indicate that the behavior at 90 °C is not very similar to the behavior of homogeneous, homopolymer liquids exhibiting linear responses for γ_0 as large as 0.5. Although not shown here, this homopolymer-like, linear behavior was observed at higher T, 100 °C.

At an intermediate temperature, $T = 50$ °C (Figure 3), the Lissajous patterns are elliptic and the moduli are independent of γ_0 only for small γ_0 ($\leq$0.05). For larger γ_0, the patterns become lozenge-shaped. For these distorted patterns, the maximum stress σ_{max} (=the σ-amplitude) is insensitive to γ_0 at low ω. In addition, plots of σ at low ω against a rescaled strain, $\tilde{\gamma} = \gamma + \gamma_0$ (=0 at a reversal point of strain), are quite insensitive to γ_0 (cf. bottom of part a, where the plots are shown for $\gamma_0 = 0.4$, 0.6, and 0.8). Thus, $\sigma(t)$ at low ω is determined only by *the rescaled strain $\tilde{\gamma}$ measured from the reversal point* and is insensitive to the oscillatory shear rate ($\propto\gamma_0$). As noted previously,[13-15] these features of $\sigma(t)$ are characteristic of plastic fluids.

To demonstrate how the plasticity leads to the lozenge-shaped Lissajous patterns having the above features, we here summarize dynamic responses of a Bingham plastic model composed of a viscous element (dashpot) connected in parallel to a yielding element (latch with yield value σ_y) and in series to an elastic element (spring). This model exhibits the lozenge-shaped patterns in the following way:[13] In each cycle of oscillatory strain, the latch locks the motion of the dashpot and the model exhibits an elastic response of the spring when $|\sigma| < \sigma_y$ at $\tilde{\gamma} \cong 0$. This response gives a γ_0-independent, steeply increasing portion of the lozenge-shaped patterns at $\tilde{\gamma} \cong 0$ (cf. Figure 3a). On the other hand, when $|\sigma|$ is increased to σ_y with increasing $\tilde{\gamma}$, the latch slides to release the motion of the dashpot. At sufficiently low ω, the dashpot has negligible contribution to σ. For this case, the sliding latch determines the stress, $|\sigma| = \sigma_y$,[13] resulting in a horizontal portion of the Lissajous patterns having γ_0- and $\tilde{\gamma}$-independent stress level (cf. Figure 3a). In summary, the lozenge-shaped Lissajous patterns seen at *low* ω result from the elastic deformation and successive plastic flow repeated twice in the opposite direction during one cycle of the oscillatory strain. This is the case not only for the Bingham model but also for plastic fluids in general. Thus, the patterns seen in Figure 3 indicate that the SIS/C14 system at 50 °C is in the plastic regime.

Figure 3 also indicates that σ_{max} at high ω gradually increases with γ_0. For this case, the distortion of the patterns becomes less significant, as is most quantitatively noted in Figure 5, where the measure of nonlinearity, R_j (with $j = 3$ and 5; cf. eq 2), determined for $\gamma_0 = 0.4$ is plotted against ω. (Representative data taken in the plastic regime are shown.) Clearly, R_j decrease with increasing ω, indicating that the contribution of higher order harmonics to σ decreases with increasing ω. For the SIS/C14 system containing polymeric components, both plastic and viscoelastic stresses contribute to the observed σ. The latter (giving only fundamental harmonics) overwhelms the former (giving all odd harmonics) at high ω, thereby reducing the relative contribution of the higher harmonics. In fact, this reduction is seen also for the Bingham model:[13] σ of the dashpot (mimicking the viscoelastic stress of the polymeric components) overwhelms σ_y of the latch at high ω to reduce the contribution of the higher harmonics.

III.2. Frequency Dependence of Moduli. Figures 6–8 show the frequency (ω) dependence of the linear moduli G' and G'' (obtained for small γ_0) and the

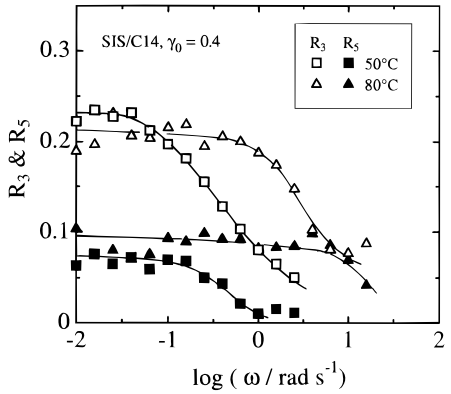

Figure 5. Frequency dependence of the measure of the nonlinearity, R_3 and R_5 for $\gamma_0 = 0.4$ (cf. eq 2), for the SIS/C14 system at 50 and 80 °C (plastic regime).

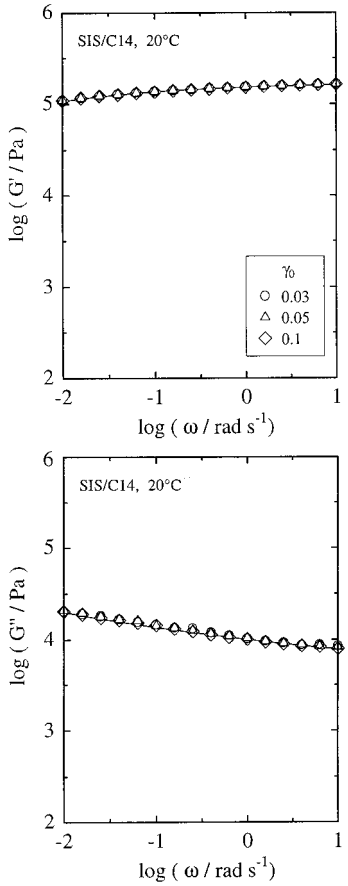

Figure 6. Frequency dependence of the linear moduli, G' and G'', for the SIS/C14 system at 20 °C (rubbery regime).

nonlinear moduli for fundamental harmonics G_1' and G_1'' (obtained for large γ_0) in the rubbery (20 °C), plastic (50 °C), and viscous (90 °C) regimes, respectively. At respective T, the data for the smallest γ_0 were reproduced after the measurements for the largest γ_0, confirming that no *irreversible* changes (in rheology and structure) were induced by those measurements.

In the rubbery regime (Figure 6), the SIS/C14 system is linear viscoelastic and the moduli are independent of γ_0: we note that G' is almost independent of ω and G'' is considerably smaller than G'. This behavior is similar to that of softly cross-linked rubbers exhibiting equilibrium elastic moduli at sufficiently low ω.

In the plastic regime (Figure 7), the behavior of the linear moduli, G' and G'' (filled circles: for $\gamma_0 = 0.05$), is essentially the same as that in the rubbery regime:

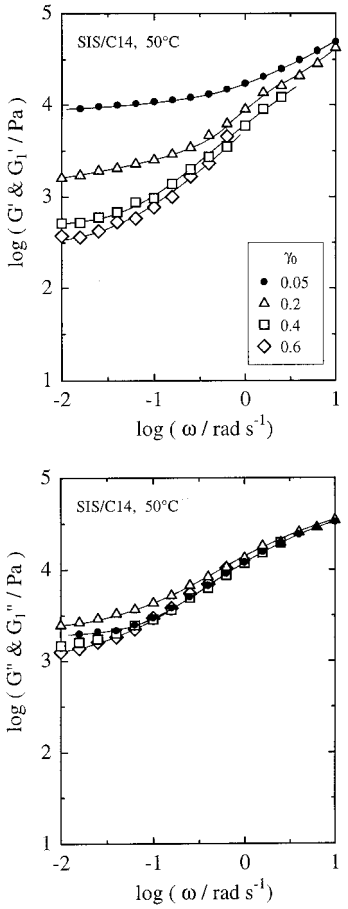

Figure 7. Frequency dependence of the linear moduli, G' and G'' (filled circles), and nonlinear moduli, G_1' and G_1'' (unfilled symbols), for the SIS/C14 system at 50 °C (plastic regime).

G' tends to level off and G'' becomes considerably smaller than G' with decreasing ω. However, with an increase in γ_0 the nonlinear modulus G_1' (unfilled symbols) decreases in particular at low ω. This behavior is similar to that of plastic, micellar solutions of diblock copolymers in selective solvents.[13−15] It should also be noted that the nonlinear G_1' and G_1'' for respective γ_0 tend to level off and approach their low-ω asymptotes.

In the viscous regime at 90 °C (Figure 8), the ω dependence of the linear G' and G'' (filled circles: for $\gamma_0 = 0.05$) is stronger than that at 50 °C and the terminal relaxation behavior ($G' \propto \omega^2$, $G'' \propto \omega$) is observed in our ω window. We also note changes of the nonlinear G_1' and G_1'' with γ_0 (unfilled symbols). The ω dependence of G_1' and G_1'' is weaker than that for G' and G''. Since G_1' and G_1'' are the nonlinear moduli, their ω dependence is not quantitatively related to a nonlinear relaxation mode distribution. However, in a qualitative sense, we may consider that the weak ω dependence of G_1' and G_1'' reflects shear-induced, extra nonlinear relaxation modes (that are slower than the linear relaxation modes seen for G' and G''). These slow nonlinear modes are discussed later in relation to the structure in the system. Although not shown here, the system exhibited linear relaxation behavior in the entire range of γ_0 and ω at higher T, 100 °C; large-γ_0 strain had no effect on the relaxation mode distribution at 100 °C.

As done in Figures 2−4 and 6−8, Lissajous patterns and the resulting moduli (G' and G'' as well as G_1' and G_1'') were examined at various temperatures to specify whether the system was in the rubbery, plastic, or

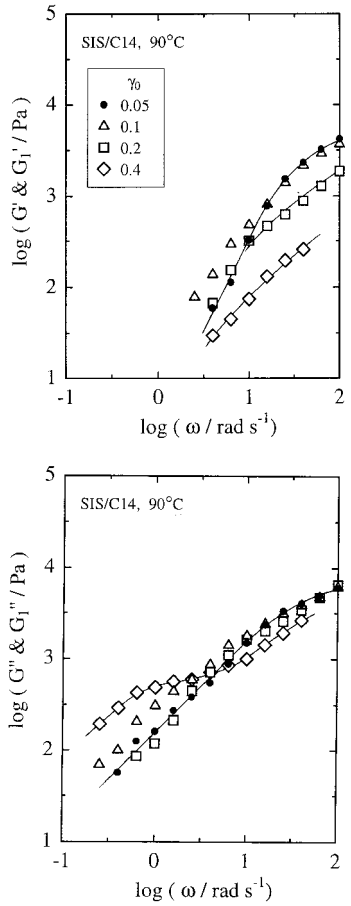

Figure 8. Frequency dependence of the linear moduli, G' and G'' (filled circles), and nonlinear moduli, G_1' and G_1'' (unfilled symbols), for the SIS/C14 system at 90 °C (viscous regime).

viscous regime. Figure 9 shows the ω dependence of those moduli obtained at the temperatures as indicated. The unfilled, half-filled, and fully filled symbols indicate that the system is in the rubbery, plastic, and viscous regimes, respectively. For the data shown in Figure 9, γ_0 is 0.4 at $T \geq 40$ °C and 0.1 at $T = 20$ and 30 °C (where slippage of the sample disturbed measurements for $\gamma_0 = 0.4$). With these γ_0, linear G' and G'' were obtained at 20, 30, and 100 °C while nonlinear G_1' and G_1'' were obtained at other temperatures.

Figure 9 demonstrates that the system exhibits a rather sharp rubbery−plastic−viscous transition with increasing T. The moduli do not obey the simple time−temperature superposition in the entire range of T. This failure of the superposition reflects structural changes that induce the rheological transition. We also note that the terminal relaxation behavior characterized with the relationships $G' \propto \omega^2$ and $G'' \propto \omega$ is finally attained for $\gamma_0 = 0.4$ at a sufficiently high temperature, $T = 100$ °C. All these results are later compared with the dielectric data to discuss structural origins for the rheological transition.

III.3. Dielectric Behavior. Figure 10 shows the changes of dielectric loss (ϵ'') curves with temperature at the quiescent state. The unfilled, half-filled and fully filled symbols indicate the data in the rubbery, plastic, and viscous regimes, respectively.

The S blocks have dipoles perpendicular to the chain contour (so-called type-B dipoles[8]) and their segmental motion can, in principle, contribute to the dielectric dispersion. However, at $T < T_g^{PS}$, this segmental motion is frozen and the S blocks are dielectrically inert.

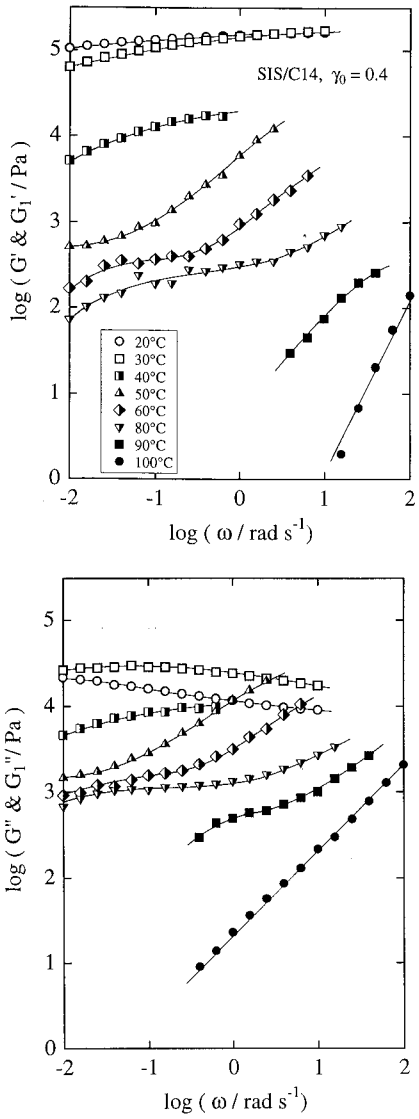

Figure 9. Frequency dependence of the linear and nonlinear moduli for the SIS/C14 system at temperatures as indicated. The unfilled, half-filled, and fully filled symbols indicate the data in the rubbery, plastic, and viscous regimes, respectively. The strain amplitude is $\gamma_0 = 0.4$ for $T \geq 40$ °C (plastic and viscous regimes) and $\gamma_0 = 0.1$ for $T = 20$ and 30 °C (rubbery regime). With these γ_0, the linear moduli, G' and G'', were obtained at 20, 30, and 100 °C while the nonlinear moduli, G_1' and G_1'', were obtained at other temperatures.

At $T > T_g^{PS}$, S blocks can contribute to the dielectric dispersion but the resulting loss is expected to be $\epsilon'' < 0.0014$ for the S blocks with the content < 15 vol % in the system. (The ϵ'' maximum value for the bulk PS segmental relaxation is $\epsilon'' \approx 0.009$.)[16] Therefore, the dispersion seen in Figure 10 is exclusively attributed to motion of the I blocks. Although the segmental motion of the I blocks is dielectrically active, this motion is detected at very high frequencies, $\omega \cong 10^7$ s^{-1} even for *bulk* I blocks at room temperature.[9] For the I blocks in the I/C14 matrix phase, the segmental friction is smaller than that in the bulk and thus the segmental relaxation should be observed at $\omega > 10^7$ s^{-1}, which is far above our experimental window. From these considerations, the dispersion observed in Figure 10 is attributed to the global motion (fluctuation of end-to-end vectors) of I blocks.

In Figure 10, the dielectric dispersion is not observed in the rubbery regime ($T \leq 30$ °C, unfilled circle). In the viscous regime ($T \geq 90$ °C, filled symols), the

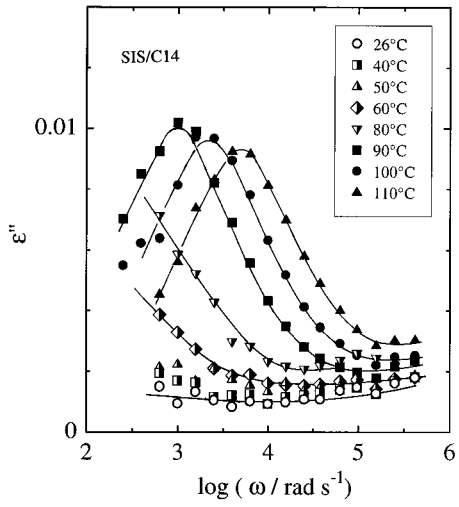

Figure 10. Dielectric behavior of the SIS/C14 system at temperatures as indicated. All data were taken at the quiescent state. The unfilled, half-filled, and fully filled symbols indicate the data taken in the rubbery, plastic, and viscous regimes, respectively.

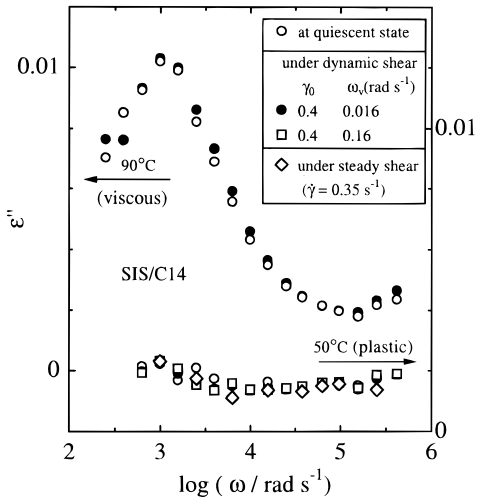

Figure 11. Comparison of the dielectric behavior at the quiescent state and under oscillatory/steady shear. Representative data in the plastic and viscous regimes are shown. At all temperatures examined, the shear had no effects on the dielectric behavior.

dispersion is clearly observed as sharp ϵ'' peaks. In this regime, the ϵ'' peaks shifts to the higher frequency side and decreases its height with increasing T, similar to dielectric changes of homopolyisoprene. In the plastic regime ($40 \leq T/°C \leq 80$, half-filled symbols), the dielectric dispersion is not observed below 50 °C. However, at higher T (≥60 °C, still in the plastic regime), the upturn of ϵ'' curves is observed at low ω. This upturn suggests the existence of dielectric dispersions at lower ω.

Figure 11 shows ϵ'' curves obtained at 50 °C (in the plastic regime) and 90 °C (in the viscous regime) under oscillatory ($\gamma = \gamma_0 \sin \omega_v t$) and steady shear. For comparison, the curves at the quiescent state are also shown (unfilled circle). The frequency of the oscillatory strain, ω_v, is much lower than ω for the dielectric measurements. Under the oscillatory shear, ϵ'' is averaged for a sufficiently long time (≫ the period of oscillatory shear), meaning that the ϵ'' data of Figure 11 represent dielectric responses of the system under plastic or viscous flow at an average shear rate, $|d\gamma/dt| = 2\gamma_0\omega/\pi$. As noted in Figure 11, neither the oscillatory nor steady shear flow affects the ϵ'' curves in the ω range examined. In fact, no shear effect was observed for ϵ'' in the entire range of T examined.

IV. Discussion

The SIS/C14 system exhibits the rubbery−plastic−viscous transition with increasing T (cf. Figures 2−4 and 6−8). A similar transition was observed for the previously studied SBS/C14 systems.[7] The dielectric dispersion of the SIS/C14 system results from motion of the I block ends and thus provides some detailed insight for the structural origins of the rheological responses: The dielectric behavior at the quiescent state corresponds to equilibrium thermal motion that determines linear viscoelastic responses, while the behavior under oscillatory/steady state detects the I block motion under the shear. Thus, comparing the rheological and dielectric data, we may discuss the structural origins of the rubbery, plastic, and viscous behavior.

IV.1. Rubbery Behavior. At low temperatures, the system exhibits rubberlike, linear viscoelastic behavior (Figures 2, 6, and 9). This behavior has been attributed to a network structure of the rigid, discrete S domains connected with rubbery I blocks.[1−7] In fact, the rubbery behavior of the SIS/C14 system is observed at $T < T_g^{PS}$, with T_g^{PS} (≅34 °C; see Experimental Section) being the glass transition temperature for the (swollen) S domains in the system. This structural assignment is consistent with the dielectric result (Figure 10): The SIS/C14 system exhibited no dielectric dispersion in the rubbery regime, indicating that the ends of the I blocks are tightly anchored on the rigid S cores and fixed in space.

IV.2. Viscous Behavior. In the viscous regime ($T \geq 90$ °C), dielectric dispersion emerges (Figure 10), and changes of the ϵ'' curve with T are similar to those for homopolyisoprene (hI). This result indicates that the thermal motion of I block ends at a quiescent state is as active as the motion of hI chain ends and thus the I block motion is practically unconstrained by the S blocks. This suggests more or less homogeneous mixing of the I and S blocks (in the disordered state). This structural assignment is consistent with the *linear* viscoelastic behavior (cf. filled circles in Figures 8 and 9): the terminal flow responses of the linear moduli, $G' \propto \omega^2$ and $G'' \propto \omega$, were observed at $T \geq 90$ °C in our ω window.

From these responses, the steady-state recoverable compliance, $J_e = [G'/G''^2]_{\omega\to 0}$, is evaluated as

$$J_e = 1.3 \times 10^{-4}\ \text{Pa}^{-1} \quad (\text{at } 90\ °\text{C}); \qquad J_e = 2.3 \times 10^{-5}\ \text{Pa}^{-1} \quad (\text{at } 100\ °\text{C}) \quad (3)$$

In general, J_e sensitively reflects the distribution of *slow, linear viscoelastic modes* that are often attributed to some sort of structure. Thus, we can examine the structure in the SIS/C14 system at the quiescent state by comparing these J_e values with J_e^{homo} of the completely homogeneous SIS/C14 system. The S blocks in the SIS chains are considerably shorter than the I blocks. As a crude approximation, we may replace the SIS chains by hI chains of the same M ($=60.2 \times 10^3$) and estimate J_e^{homo}. A reduced molecular weight of those hI chains, $cM = 24.5 \times 10^3$ (c = concentration in mass/volume), is significantly smaller than the characteristic molecular weight ($=60 \times 10^3$)[17] for appearance of entanglement effects for J_e of bulk hI. Thus, we may use the Rouse equation[17] to evaluate J_e^{homo} as

$$J_e^{homo} = 2M/5cRT \cong 1.9 \times 10^{-5}\ Pa^{-1} \quad (\text{at } T = 90-100\ °C) \quad (4)$$

At 90 °C, the measured J_e is considerably larger than J_e^{homo}. Thus, at this temperature the disordered SIS/C14 system appears to have some *dynamic* structure that leads to the slow, linear viscoelastic modes. This dynamic structure may be related to the concentration fluctuation pattern[18] near the order−disorder transition. At higher T, 100 °C, J_e agrees well with J_e^{homo}, and the system appears to be in a completely homogeneous state with neglible fluctuation.

The above argument is supported from comparison of viscoelastic and dielectric terminal relaxation times, τ_G and τ_ϵ, the latter detecting the global motion of *individual* chains. τ_G is defined as $\tau_G = J_e\eta_0$, with $\eta_0 = [G''/\omega]_{\omega\to 0}$ being the zero-shear viscosity.[17] When ϵ'' exhibit a sharp peak (as is the case for the SIS/C14 system at $T \geq 90$ °C), we can define τ_ϵ as $\tau_\epsilon = \omega_p^{-1}$, with ω_p being the angular frequency for the peak. From the G^* data (filled circles in Figures 8 and 9), we find

$$\tau_G = 2.0 \times 10^{-2}\ s \quad (\text{at } 90\ °C); \qquad \tau_G = 5.2 \times 10^{-4}\ s \quad (\text{at } 100\ °C) \quad (5)$$

The ϵ'' data (Figure 10) give

$$\tau_\epsilon \cong 1.0 \times 10^{-3}\ s \quad (\text{at } 90\ °C); \qquad \tau_\epsilon \cong 4.6 \times 10^{-4}\ s \quad (\text{at } 100\ °C) \quad (6)$$

At 100 °C, τ_G is close to τ_ϵ and thus the linear viscoelastic, terminal relaxation corresponds to the global motion of individual chains. This result suggests negligible fluctuation effects for G^* at 100 °C. On the other hand, at 90 °C, τ_G is significantly longer than τ_ϵ and the linear viscoelastic relaxation appears to correspond to the fluctuation process (slower than the motion of individual chains).

The nonlinearity of G_1' and G_1'' at 90 °C (Figure 8) might also be related to the fluctuation effect. As explained for Figure 8, the large-amplitude shear strain may provide some *nonlinear* relaxation modes (slower than the linear modes) to the system. If the fluctuation existing at the quiescent state (or under small strain) is suppressed by the large strain, some sort of strain-induced structure may emerge in the system to provide such slow nonlinear modes.[19]

IV.3. Plastic Behavior. The rubbery to plastic transition takes place between 30 and 40 °C (Figure 9). This transition temperature is close to T_g^{PS} (≅34 °C) for the (swollen) S domains in the system. Thus, the plastic behavior appears to prevail when the S domains become a softened, viscoelastic liquid. However, the thermal motion of I blocks at the quiescent state is not active enough to spontaneously pull the S blocks out from S domains into the enthalpically unfavorable I/C14 matrix. Thus, at the quiescent state, motion of the I block ends appears to be limited in the thickened S/I interface. The onset of dielectric dispersion (upturn of ϵ'' at low ω) seen at the quiescent state in the high-T part of the plastic regime (Figure 10) may be attributed to this motion in the interface (that is enhanced at higher T).

Now, we consider the mechanism of plastic flow of the SIS/C14 system against large strain (cf. lozenge-shaped patterns in Figure 3). A previous study attributed the plasticity of SBS/C14 systems (similar to the present SIS/C14 system) to the pullout of S blocks from S domains by the middle (B) blocks being strained and stretched by the shear.[7] As explained earlier, this chain pullout process can certainly provide the plastic to the system. For this process, the simplest expectation is that the system becomes dielectrically active under large shear because the end-to-end vectors of the I blocks can fluctuate when the S blocks are pulled out. However, the experiments indicate no shear effect on ϵ'' (Figure 11). This difference between the observation and the expectation suggests three possibilities.

The first possibility is that the S blocks pulled out in the I/C14 phase have much larger friction than the I blocks, thereby retarding the motion of the I block ends (connected to the S blocks) and locating the dispersion of the I blocks at low ω not covered in our experiments. This large friction of the S blocks may be realized in particular when a few, pulled out S blocks coagulate in the I/C14 phase.

The second possibility is related to heterogeneous flow in the SIS/C14 system. Quiescently ordered block copolymer systems are usually composed of many grains,[20] and the flow may take place mainly at grain boundaries. If this is the case for our SIS/C14 system, only a small fraction of the I blocks located at the grain boundaries will pull out the S blocks. Then, the dielectric intensity associated with the pullout of the S blocks may become nondetectably weak.

The third, interesting possibility (not considered in the previous work[7]) is related to two conformations available for the I block, a bridge connecting different S domains and a loop having two ends on the same S domains:[11] The applied strain effectively stretches the bridge-type I block to pull out the S blocks and could induce dielectric dispersion. On the other hand, the loop is not significantly stretched and thus the S blocks connected to the loops are not easily pulled out, resulting in strain-insensitive ϵ''. Therefore, if the fraction of the bridge is small, the dielectric behavior is not much affected by the strain. In fact, for a lamellar system of a bulk SIS copolymer, the bridge fraction has been estimated to be ≅40% and thus the bridge is not the dominant conformation for the I blocks.[11]

Concerning the above argument, we note that the loop can also provide the plasticity to the SIS/C14 system through a mechanism similar to that for concentrated C14 solutions of SI and/or SB diblock copolymer micelles.[13−15] In these solutions, spherical micelles with glassy S cores and a solvated I or B corona are overlapping with each other to form regular, cubic lattices called macrolattices.[13−15] The macrolattice provides plasticity to the solutions; it deforms elastically against stress smaller than the lattice strength σ_y while it flows (without rupture of the micelles) when the stress exceeds σ_y. The driving force of the macrolattice formation is in turn related to the thermodynamic confinements for the corona blocks.[13−15] In the micellar solution, the corona blocks are required to have a uniform concentration distribution in the C14 matrix phase to reduce an osmotic free energy. At the same time, each corona block is required to have randomized conformations to reduce an elastic free energy. For the corona blocks tethered on rigid S cores, these osmotic and elastic requirements are opposite one another: For the concentration to be completely uniform in the matrix, the corona blocks of neighboring micelles should have highly correlated conformations and thus have a small conformational freedom. To make a compromise of those requirements, the micelles form the spatially

symmetric macrolattice that minimizes the osmotic constraint for the conformation of individual corona blocks.[13−15] Thus, the thermodynamic confinement due to the osmotic and elastic requirements for the corona blocks is the origin of the plasticity for the micellar solutions.

Obviously, the I or B corona blocks in the diblock copolymer solutions only take a tail conformation and do not chemically connect different S cores. In this sense, the loop in the present SIS/C14 system is similar to the tail in the SI or SB solutions. Therefore, similar to the SI and SB solutions, the thermodynamic confinement due to the osmotic and elastic requirements for the loop can provide the plasticity to the SIS/C14 solution.

As discussed above, the plasticity of the SIS/C14 solution can be attributed to two different mechanisms, "pullout of S blocks" for the bridge I blocks and "thermodynamic confinement" for the loops. The shear-insensitive dielectric responses (Figure 10) suggest that the latter mechanism is as important as the former. Of course, the loop exhibits *plasticity* only when the system *flows*: For small strain, the system does not flow and the loop exhibits an essentially elastic response (the behavior before yielding). This elastic response of the loop may have contributed also to G' and G'' of the SIS/C14 system in the rubbery regime. Thus, as long as the system has bridges (even as the minor component), the plasticity of loops would emerge only when the bridges pull out the S blocks. In other words, bridges determine whether the loop provides elasticity or plasticity.

V. Concluding Remarks

The SIS/C14 system exhibits the rubbery−plastic−viscous transition with increasing temperature. Comparison of rheological and dielectric data indicates that the rubbery behavior at low T corresponds to a network structure of the glassy S domains connected with rubbery I blocks, while the viscous behavior at high T corresponds to more or less homogeneous mixing of the S and I blocks and active thermal motion of the I block ends. These assignments are in harmony with the previous discussion. However, this study reveals a possibility that the thermodynamic confinement (compromise of the osmotic and elastic requirements) for the loop-type I blocks may have a large contribution to the plasticity of the system. Thus the previously considered mechanism for the plasticity, pullout of the S blocks from the S domain due to tension along I bridges, is not the only possible mechanism. From this point of view, it is desirable to evaluate the bridge fraction in the SIS/C14 system and examine the loop contribution to the plasticity. An attempt is now being made, and the results will be presented in our next paper.

Acknowledgment. We acknowledge with thanks the financial support for this study from the Ministry of Education, Science, Sports and Culture, Japan, under Grant No.08875194.

References and Notes

(1) Holden, G.; Bishop, E. T.; Legge, N. R. *J. Polym. Sci.* **1969**, *C26*, 37.
(2) Chung, C. I.; Gale, J. C. *J. Polym. Sci., Polym. Phys. Ed.* **1976**, *14*, 1149.
(3) Chung, C. I.; Lin, M. I. *J. Polym. Sci., Polym. Phys. Ed.* **1978**, *16*, 545.
(4) Chung, C. I.; Griesbach, H. L.; Young, L. *J. Polym. Sci., Polym. Phys. Ed.* **1980**, *18*, 1237.
(5) Pico, E. R.; Williams, M. C. *Polym. Eng. Sci.* **1977**, *17*, 573.
(6) Gouinlock, E. V.; Porter, R. S. *Polym. Eng. Sci.* **1977**, *17*, 535.
(7) Watanabe, H.; Kuwahara, S.; Kotaka, T. *J. Rheol.* **1984**, *28*, 393.
(8) (a) Stockmayer, W. H. *Pure Appl. Chem.* **1967**, *15*, 539. (b) Baur, M. E.; Stockmayer, W. H. *J. Chem. Phys.* **1965**, *43*, 4319. (c) Stockmayer, W. H.; Burke, J. J. *Macromolecules* **1969**, *2*, 647.
(9) Adachi, K.; Kotaka, T. *Prog. Polym. Sci.* **1993**, *18*, 585.
(10) Watanabe, H.; Urakawa, O.; Kotaka, T. *Macromolecules* **1993**, *26*, 5073; **1994**, *27*, 3525.
(11) Watanabe, H. *Macromolecules* **1995**, *28*, 5006.
(12) See, for example: Molau, G. E. In *Block Copolymers*; Aggarwal, S. L., Ed.; Plenum Press: New York, 1970.
(13) Watanabe, H.; Kotaka, T.; Hashimoto, T.; Shibayama, M.; Kawai, H. *J. Rheol.* **1982**, *26*, 153.
(14) Watanabe, H.; Kotaka, T. *J. Rheol.* **1983**, *27*, 223.
(15) Watanabe, H.; Kotaka, T. *Polym. Eng. Rev.* **1984**, *4*, 73.
(16) Yano, O.; Wada, Y. *J. Polym. Sci., Part A-2* **1971**, *9*, 669.
(17) Graessley, W. W. *Adv. Polym. Sci.* **1974**, *16*, 1.
(18) Fredrickson, G. H.; Helfand, E. *J. Chem. Phys.* **1987**, *87*, 697.
(19) In fact, for symmetric polyolefin[20a] and SI[20b] diblock copolymers, large-amplitude oscillatory shear induces lamellae formation at $T >$ the quiescent ODT temperature (although the direction of the lamellar orientation is different for those copolymers).
(20) (a) Koppi, K. A.; Tirrell, M.; Bates, F. S. *Phys. Rev. Lett.* **1993**, *70*, 1449. (b) Balsara, N. P.; Hammouda, B.; Kesani, P. K.; Jonnalagadda, S. V.; Straty, G. C. *Macromolecules* **1994**, *27*, 2566.

MA960060I